Organic & Biomolecular Chemistry

Cite this: *Org. Biomol. Chem.*, 2012, **10**, 3033

www.rsc.org/obc

PAPER

Synthesis and photophysical evaluation of a pyridinium 4-amino-1,8-naphthalimide derivative that upon intercalation displays preference for AT-rich double-stranded DNA†

Swagata Banerjee, Jonathan A. Kitchen, Thorfinnur Gunnlaugsson* and John M. Kelly*

Received 10th November 2011, Accepted 26th January 2012
DOI: 10.1039/c2ob06898b

The synthesis, characterisation and solid state crystal structure of a cationic 4-amino-1,8-naphthalimide derivative (**1**) are described. The photophysical properties of **1** are shown to vary with the solvent polarity and H-bonding ability. The fluorescence of **1** is enhanced and blue-shifted in its 1 : 1 complex with 5′-adenosine-monophosphate while it is partially quenched and red-shifted in its complex with 5′-guanosine-monophosphate. Linear and circular dichroism measurements show that **1** binds to double-stranded DNA by intercalation. Comparative UV-visible and fluorescence studies with double stranded synthetic polynucleotides poly(dA–dT)$_2$ and poly(dG–dC)$_2$ show that **1** binds much more strongly to the AT polymer; **1** also has a strong preference for A–T rich sequences in natural DNA. Thermal denaturation measurements also reveal a much greater stabilisation of the double-stranded poly (dA–dT)$_2$ than of natural DNA.

Introduction

The development of small molecules capable of binding to DNA and exhibiting anticancer activities has received much attention in recent times.[1–3] 1,8-Naphthalimide derivatives represent an important family of DNA binders that have been shown to exhibit anti-tumour activities *in vitro* and *in vivo*.[4,5] Moreover, the naphthalimides have rich photophysical properties; which are dependent on the nature, as well as the location, of any aryl substituents. Photo-excitation of various naphthalimide derivatives has been also shown to induce sequence selective DNA strand cleavage.[6–8] For example, Saito *et al.* showed that unsubstituted as well as 4-nitro substituted L-lysine derived 1,8-naphthalimides caused sequence selective cleavage at the 5′-guanine (G) residue of 5′-GG sequence upon UV-irradiation and treatment with hot piperidine. The cleavage ability of these naphthalimide systems has been explained in terms of photoinduced electron transfer (PET), occurring from the most oxidizable DNA base G, to the triplet excited state of naphthalimide.[6] In a related study, Kelly and co-workers have reported the interaction of cationic unsubstituted naphthalimides functionalised with *N*-ethyl pyridinium group, with DNA and mononucleotides[8] and showed that laser flash photolysis could be employed to observe the formation of naphthalimide radical anion (NI$^{\bullet-}$) in the presence of DNA.

While these unsubstituted naphthalimides absorb only at shorter wavelength, the 3- and 4-amino-1,8-naphthalimide derivatives by contrast absorb within the visible region (λ_{max} ~ 450 nm) and fluoresce at long (λ_{max} ~ 550 nm) wavelengths, with reasonably high quantum yield of emission in various organic and aqueous solvents.[9] Because of this, they have been extensively explored for the development of sensors for biologically relevant ions and molecules, *etc*.[9–16] Their excited states are characterized by a "push–pull" internal charge transfer (ICT) character, arising from the presence of the electron-withdrawing imide and the electron donating amino moiety; this being strongest where the amino group is in the 4-position of the ring.[9,15–19] Because of this they have also been employed as potential cellular imaging and antitumor agents.[20] In this context, we have also reported development of DNA photocleavage agents based on 4-amino-1,8-naphthalimide conjugated with ruthenium(II) complex,[19] and we have prepared Tröger's base derivatives of the 4-amino-1,8-naphthalimide structure and shown these to be efficient DNA binders, and cytotoxic agents.[20] In this article we report the synthesis of **1** (a novel cationic pyridinium based 4-amino-1,8-naphthalimide derivative), and examine its interaction with natural and synthetic double-stranded DNAs using UV-visible absorption, fluorescence, linear and circular dichroism spectroscopic methods. These demonstrate that unlike its unsubstituted analogue **2**, the 4-amino-substituted compound **1** intercalates into double-stranded DNA and shows an apparent preference for AT sites.

School of Chemistry, Centre of Synthesis and Chemical Biology, University of Dublin, Trinity College Dublin, Dublin2, Ireland. E-mail: jmkelly@tcd.ie, gunnlaut@tcd.ie; Tel: +3531 896 1947+353 1 896 3459

†Electronic supplementary information (ESI) available: Fig. S1–S3. CCDC 843421. For ESI and crystallographic data in CIF or other electronic format see DOI: 10.1039/c2ob06898b

Results and discussion

Design, synthesis and solid state characterisation of 1

In designing the molecule we foresaw that in **1** the pyridinium moiety would impart water solubility as well as favouring, electrostatic interaction with the negative phosphate backbone of the DNA. The substitution should also prevent protonation in the pH range used for studies with the biomolecule, simplifying the spectroscopic studies.

Compound **1** was synthesised in three steps as shown in Scheme 1.[8,21] The first step involved formation of **3**, which was achieved through a condensation reaction between the 4-nitro-1,8-naphthalic anhydride and ethanolamine in dry ethanol under an inert atmosphere and reflux.[21] Product **3** was isolated as a brown solid in 75% yield and fully characterised (see ESI Fig. S1†). Compound **4** was then formed, as an orange solid in 90% yield by catalytic hydrogenation of **3** using 10% Pd/C in DMF at 3 atm H_2. Refluxing **4** in the presence of *p*-toluene sulfonyl chloride in pyridine, gave the desired product **1** as a tosylate salt. This was put into water, washed with CH_2Cl_2 and purified using silica flash column chromatography (88 : 11 : 1 $CH_3CN : H_2O : NaCl$). The product was then precipitated as its PF_6^- salt using NH_4PF_6 and converted to the chloride salt of **1** by the treatment with DOWEX-1 × 8–200 ion exchange resin. All compounds were characterized by conventional ^1H, ^{13}C NMR (see ESI Fig. S2†), HRMS and IR techniques.

Large orange, X-ray quality crystals of **1** were obtained as the PF_6^- salt from acetone.† The low temperature (112 K) structure of **1** is shown in Fig. 1a, where it can be seen that the pyridinium ring is oriented towards the top face of the naphthalimide ring as the ethylene linker adopts a gauche conformation, placing the pyridinium moiety over one of the oxygen atoms of the imide structure. This is probably a consequence of the electron deficient nature of the pyridinium ring and the electron rich imide portion of the naphthalimide ring. Indeed, Gao and Marcus showed that this 'push–pull' character places a partial positive charge on the 4-amino moiety and a partial negative charge at the imide site causing the charge to be distributed on the carbonyl portions of the imide and making the central nitrogen moiety electron deficient.[22] This might explain the orientation of the pyridinium ring in Fig. 1a. The packing interactions of **1** were found to be governed by N–H hydrogen, anion···π interactions and π···π stacking. H-bonding interactions between the amino proton on one molecule and the carbonyl oxygen atom on an adjacent molecule give rise to a 1D polymeric chain in the crystallographic *a*-direction [N(1)···O(1) = 2.919(3) Å and <(N(1)–H(1X)···O(1)) = 154°]. π···π stacking [centroid···centroid = 3.595 Å] between naphthalimide moieties on an adjacent chain links the chains in an anti-parallel (head-to-tail) fashion (as shown in Fig. 1b). The PF_6^- counter anion is also involved in H-bonding [N(1)···F(5) = 3.304(3) Å and <(N(1)–H(1Y)···F(5)) = 139°] and anion···π interactions (F···centroid = 3.241 Å) further extending the packing.

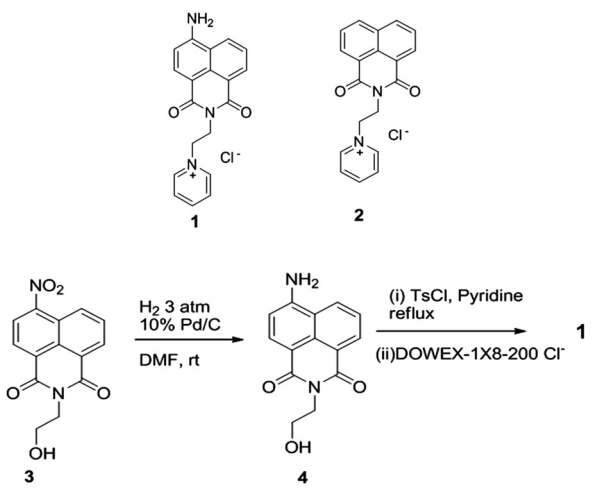

Scheme 1 Synthesis of **1**.

UV-visible, fluorescence and NMR studies of 1

The absorption and emission spectra of **1** (8.3 μM) in 10 mM phosphate buffer solution (pH 7.0) are shown in Fig. 2a. **1** exhibits a broad absorption band 435 nm (ε = 13 200 M^{-1} cm^{-1}), which is, as discussed above, due to an ICT transition.[9,23,24] Higher energy π–π* transitions were also observed at wavelength *ca.* 250 nm (ε = 21 800 M^{-1} cm^{-1}). In the same solvent (pH 7.0), **1** exhibits a broad ICT fluorescence emission band centred at 552 nm, when excited at 435 nm. As anticipated the photophysical properties of **1** were found to be pH independent in the range pH 3–11 (see ESI, Fig. S3†), which is useful for its application as a DNA targeting molecule.

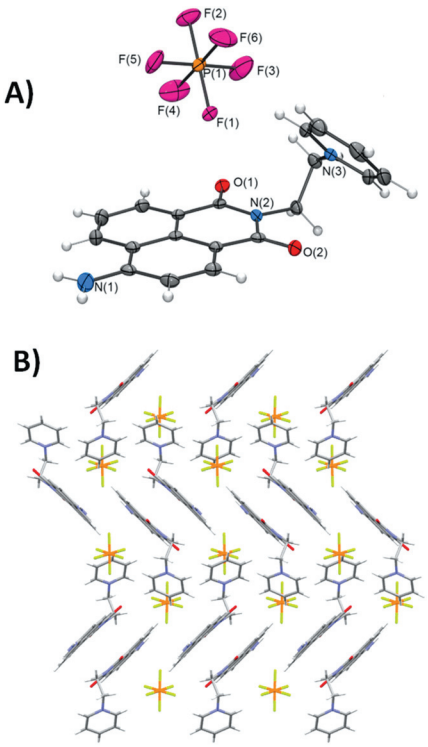

Fig. 1 (A) The X-ray crystal structure of **1** with thermal ellipsoids shown at 50% probability. (B) The packing of **1** when viewed down the crystallographic *a*-axis, showing the π–π interactions between the stacked naphthalimide rings which adopt a 'head-to-tail' type orientation.

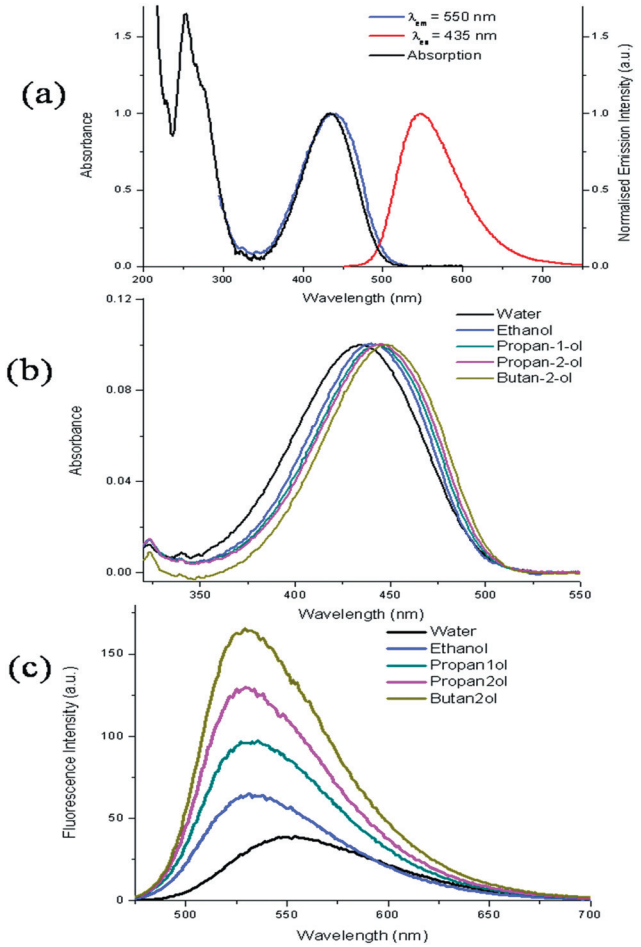

Fig. 2 (a) Normalised UV-vis (—), fluorescence spectra (–) λ_{ex} = 435 nm and excitation spectra (–) λ_{emx} = 550 nm of **1** in 10 mM phosphate buffer (pH 7). (b) The absorption and (c) the emission spectra of **1** in different solvent of varying polarity.

Compound **1** shows good water solubility, and obeys the Beer–Lambert law in aqueous solution at concentrations up to 100 μM as expected if the molecule exists in its monomeric form under these conditions. However, as we wish to study the compound in higher concentrations in further studies (*e.g.* cellular studies), it was important to determine whether the compound might aggregate under such conditions. To investigate this we carried out ^{1}H NMR studies (600 MHz, D_2O) within the concentration range of 1 μM → 10 mM. These showed (see ESI†) that the naphthalimide ring protons were shifted upfield upon increasing concentration above 100 μM (even though no new band was observed in the UV/vis absorption spectrum). The NMR results are consistent with the formation of small aggregates at these higher concentrations. This is not too unexpected given the ability of **1** to undergo π–π stacking as was observed in the solid state structure in Fig. 1. Importantly, these results also show that the compound is monomeric at the concentrations of **1** employed in the photophysical studies herein.

To investigate the effect of solvent polarity, the absorption and fluorescence emission spectra of **1** were recorded in alcohols of varying polarity as well as in water. Representative spectra are shown in Fig. 2, and the results are summarised in Table 1. In all the solvents, **1** exhibited a broad absorption band, which showed a slight blue shift (*ca.* 8–9 nm) on moving from the less polar butan-2-ol to highly polar water. The emission properties were found to be much more strongly dependent on the polarity of the medium, showing *ca.* 22 nm red shift on moving from butan-2-ol to water and a significant decrease in the quantum yield of emission and fluorescence lifetime. The radiative (k_r) and non radiative (k_{nr}) decay constants were estimated from the quantum yield and lifetime values, respectively. This showed that for the alcohols k_r is not significantly altered with increase in solvent polarity, while k_{nr} increased substantially between butan-2-ol and ethanol. By contrast in water, k_r was found to be significantly lower compared to the alcohols.

Table 1 UV-vis absorption and emission data for **1** in a range of solvents

Solvent	λ_{max} (Abs) (nm)[a]	λ_{max} (Flu) (nm)[a]	ϕ_F	τ (ns)[a]	k_r(×10^7) (s^{-1})	k_{nr}(×10^8) (s^{-1})
Water	436	552	0.08	2.25	3.6	4.0
Ethanol	440	536	0.16	2.60	6.1	3.2
Propan-1-ol	444	534	0.23	3.21	7.2	2.4
Propan-2-ol	444	532	0.29	3.90	7.43	1.8
Butan-2-ol	445	530	0.40	5.10	7.8	1.2

[a] All spectra were recorded at optical density (OD) of ~0.1 upon excitation at λ_{max} for each of these solvents.

Similar behaviour has previously been observed for related 4-amino-1,8-naphthalimides, which suggests that the excited states of these molecules have ICT character.[23–25] The decrease of quantum yield of emission and lifetime in more polar and H-bonding solvents can be explained in terms of specific solvent–solute interactions resulting in the increase in non radiative decay rates. Since **1** exhibits significant solvatochromism and as its emission quantum yield is strongly dependent on solvent polarity we may expect to observe substantial changes in the photophysical properties of **1** upon binding to nucleic acids.[26]

Interaction of 1 with mononucleotides

Ground state interaction of 1 with mononucleotides. We first investigated its ability to bind mononucleotides. As can be seen from Fig. 3a and 3b the UV-vis spectrum of **1** is significantly altered in the presence of purine mononucleotides adenosine 5′-monophosphate (AMP) (0 → 120 mM) and guanosine 5′-monophosphate (GMP) (0 → 60 mM). Addition of both AMP and GMP caused a decrease in the absorbance of **1**, with a concomitant red shift of the λ_{max}. However, the extent of hypochromicity was different with each mononucleotide (Table 2).

A single isosbestic point was observed with both AMP and GMP, suggesting the formation of 1 : 1 supramolecular ground state complex between **1** and either of the purine mononucleotides. Similar behaviour has been previously observed for unsubstituted naphthalimides and has been attributed to naphthalimide–nucleotide stacking interactions.[8] In contrast, the pyrimidine mononucleotides, cytidine 5′-monophosphate (CMP) and thymidine 5′-monophosphate (TMP) did not cause any significant change in the UV-vis spectrum of **1**.

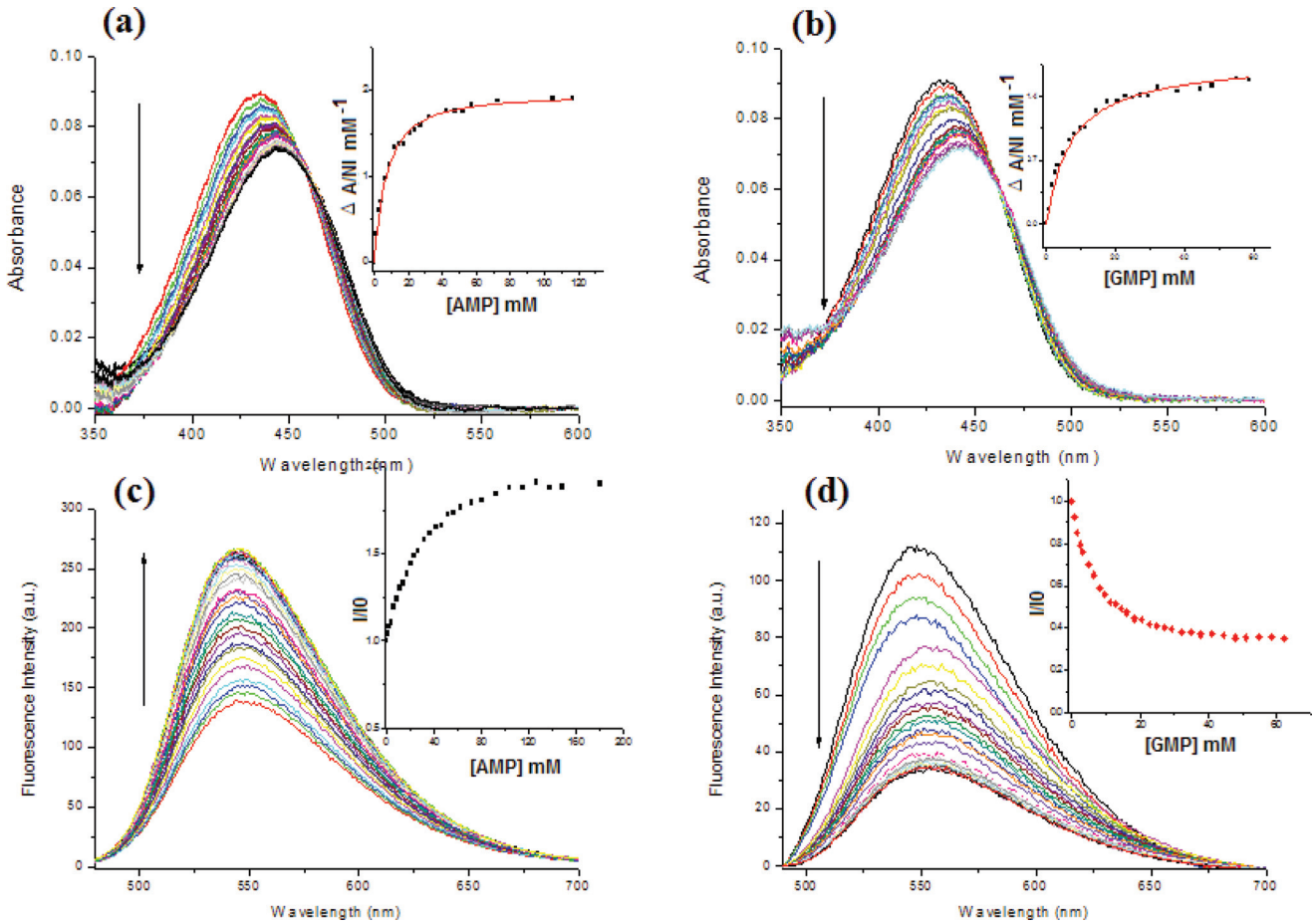

Fig. 3 Changes in the absorption spectrum of **1** (7.2 μM) in the presence of increasing concentration of (a) AMP (0–120 mM) in 10 mM phosphate buffer (pH 7.0), (b) GMP (0–60 mM). Inset: plot of $\Delta A/[NI]$ *vs.* concentration of AMP/GMP and fit (—) according to eqn (3) ($\Delta A = \lambda_{max}$ of free **1**). Changes in the steady state emission spectra of **1** (7.2 μM) in the presence of increasing concentration of (c) AMP (0–120 mM) (λ_{ex} = 463 nm) and (d) GMP (0–60 mM) (λ_{ex} = 470 nm) in 10 mM phosphate buffer (pH 7.0). Inset: plot of I/I_0 *vs.* concentration of XMP.

Table 2 Summary of binding parameters obtained from absorption spectra of **1** in presence of AMP and GMP

		Binding constant (Scatchard plot)[27]		Binding constant (nonlinear model of Deranleau)[28]	
XMP	% Hypo	K_1 (M^{-1})	K_2 (M^{-1})	K_1 (M^{-1})	K_2 (M^{-1})
AMP	19	138 ± 10	37 ± 5	155 ± 7	35 ± 5
GMP	12	117 ± 11	—	135 ± 5	—

Assuming a 1 : 1 association between **1** and the nucleotide monophosphates (XMP), the association constants for their formation were first determined using linear Scatchard analysis (see ESI† for details).[27] Good linearity was observed for the association of **1** with GMP. However, for the interaction of **1** with AMP, deviation from linearity was observed at higher nucleotide concentration, which possibly indicates that higher order supramolecular complexes also exist under these conditions. The binding data were therefore also analysed using the nonlinear expression developed by Deranleau (see eqn (3), ESI†) considering the formation of 1 : 1 and 1 : 2 complexes between **1** and XMP as shown in eqn (1).[28] The derived binding constants (Table 2) indicates that **1** complexes more strongly to AMP than to GMP. Furthermore, these are almost twice as high as that previously observed for the unsubstituted naphthalimide derivative **2**,[8b] clearly demonstrating the importance of the ICT character,

$$\mathbf{1} + \mathrm{XMP} \overset{K_1}{\rightleftharpoons} \mathbf{1} : \mathrm{XMP} \overset{K_2}{\rightleftharpoons} \mathbf{1} : (\mathrm{XMP})_2 \qquad (1)$$

which makes **1** highly polar and as such more capable of π–π stacking with these mononucleotides.

Singlet excited state interactions with mononucleotides. Having established a strong association of **1** with AMP and GMP in the ground state, we next evaluated changes in the excited state of **1**. A significant *blue* shift (7 nm) in the emission maximum is observed for **1** in the presence of AMP (120 mM) (Fig. 3c) and concurrently the quantum yield of emission of **1** (Φ_{free} = 0.08) is approximately doubled (Φ_{bound} = 0.14) when excited at the isosbestic point (λ_{ex} = 463 nm). This behaviour was further supported by time resolved fluorescence measurements, as the fluorescence lifetime increased from 2.2 ns for free **1** to 4.8 ns in the presence of AMP (70 mM), Table 3. The increase in relative quantum yield of emission and singlet state lifetime of **1** in its AMP complex can be attributed primarily to a decrease of the

Table 3 Fluorescence lifetime data as a function of mononucleotide concentration in 10 mM phosphate buffer (pH 7)

	[XMP] (mM)	ϕ_F	λ_{max} (Flu) (nm)	τ_1 (ns)	τ_2 (ns)
1	0	0.08	552	2.2 (100%)	—
1 + GMP	66	0.02	556	1.9 (33%)	0.7 (67%)
1 + AMP	71	0.14	545	2.6 (29%)	4.8 (71%)

rate of non radiative decay processes as it is less accessible to solvent molecules and is in a relatively more rigid orientation. Similar changes in non radiative decay processes have been reported for the interaction of various porphyrin[2a] and ethidium bromide derivatives with nucleobases and DNA.[29–31]

In contrast to what is found for AMP, addition of GMP (up to 60 mM) caused a *red* shift of 4 nm in λ_{max} and about 60% quenching of the emission intensity of **1** when excited at 470 nm (Fig. 3). This may be attributed to PET from guanine to the photo-excited naphthalimide moiety in the preformed complex, as has been for other naphthalimides.[8b,c] Quenching of the emission intensity of **1** at lower concentration of GMP occurs in a 1 : 1 complex. The residual fluorescence at very high concentration of GMP, where **1** is completely bound can be explained by considering fluorescence emission from the NI : GMP complexes. At very high concentration of GMP, formation of higher order complexes cannot be ruled out.

The nature of the interaction of **1** with GMP was also supported by time correlated single photon counting measurements. In aerated 10 mM phosphate buffer the fluorescence of **1** decays by single exponential kinetics with a lifetime of 2.2 ± 0.2 ns, while in the presence of GMP, two components are observed. The first one has a lifetime of *ca.* 2 ns and the second one has a lifetime of 0.7 ± 0.1 ns. The relative contribution of this short-lived component increased with increasing concentration of GMP up to 66 mM. This short-lived component is presumed to arise from a 1 : 1 excited state complex between **1** and GMP. However, it is intriguing to note that at the highest concentration used, the long-lived component (1.9 ns) still represents 33% of the emitting species, even though calculations from the UV-vis absorption titrations suggest that the concentration of free **1** should be much lower. A possible explanation is that this emitting species is **1** : $(GMP)_2$*. A longer lifetime for the **1** : $(GMP)_2$* would be similar to the behaviour recently reported for Pt(II)(meso-tetrakis(4-*N*-methyl-pyridyl))porphyrin, where the Por$(GMP)_2$* has a lifetime approximately five times longer than that for the 1 : 1 Por(GMP)* excited state.[2a]

The fluorescence enhancement of **1** in the presence of AMP is in contrast to the behaviour of the corresponding unsubstituted naphthalimide **2**, where the steady state emission of the naphthalimide derivative was quenched in the presence of both AMP and GMP.[8b] This was suggested to be due to PET from the nucleotide to the photoexcited naphthalimide chromophore. The failure to observe fluorescence quenching of **1** with AMP is presumably a consequence of the lower reduction potential of the excited state of the 4-amino derivative compared to the unsubstituted analogue, **2**.[32]

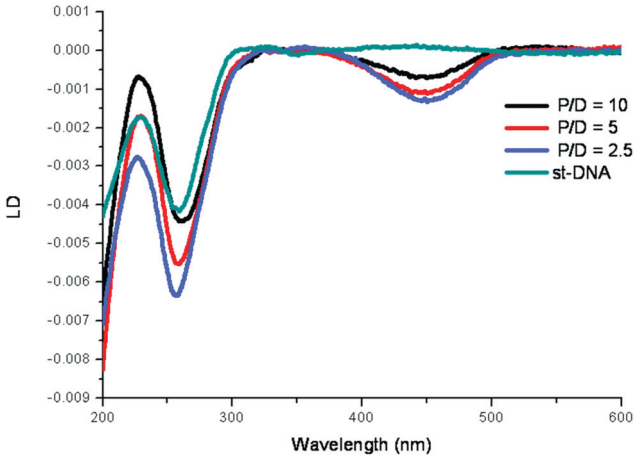

Fig. 4 The LD spectrum of free *st*-DNA (400 μM) and *st*-DNA in presence of **1** at varying P/D in 10 mM phosphate buffer (pH 7.0).

Interaction of 1 with *st*-DNA

Having explored the ability of **1** to interact with mononucleotides, we next explored the binding of **1** to double stranded salmon testes DNA (*st*-DNA) using various spectroscopic techniques, including LD, CD, UV-vis absorption and fluorescence spectroscopy, as well as thermal denaturation.

Linear dichroism measurements. LD spectroscopy, which is increasingly being found to be a powerful method for probing the binding of small molecules to nucleic acids,[33] was used to investigate the mode of binding of **1** to *st*-DNA. The DNA was flow-oriented in a Couette cell at 2000 rpm. The spectrum of free *st*-DNA (400 μM) exhibits a negative LD signal around 260 nm characteristic of B-DNA, which arises from the orientation of transition dipole of the base pairs approximately perpendicular to the helical axis of DNA. The reduced linear dichroism {LD^r = LD/(isotropic absorbance)} was calculated to be −0.027 ± 0.003 (a value similar to that obtained for B-DNA samples by other researchers[33]). The LD was also measured for *st*-DNA in the presence of **1** at nucleotide/drug ratio P/D = 2.5, 5 and 10, Fig. 4. Most significantly, a new negative band appears at 440 nm corresponding to the ICT absorption band of **1**. The reduced LD for this feature for the P/D = 5 sample is 0.033 ± 0.003, which is similar to that of the DNA sample, indicating that the naphthalimide is at approximately the same angle to the direction of flow as the base-pairs. This is as would be expected for an intercalative mode of binding by the naphthalimide (This calculation assumes that the orientation factor *S* is the same for both DNA and the naphthalimide–DNA sample. It is possible that the interaction of **1** slightly stiffens the biomolecule and hence improves the orientation of the DNA molecules along the direction of flow, which would lead to a slightly higher LD^r). At P/D = 2.5 unbound ligand makes a significant contribution to the overall absorbance value, thereby making LD^r for the 440 nm band quite low compared to the nucleobase.

Circular dichroism measurements. CD spectroscopy[33] was also used to investigate the mode of interaction of **1** with *st*-DNA (150 μM) (Fig. 5) by monitoring the changes in the CD spectrum upon addition of increasing amounts of **1** (P/D = 0 →

20). The ellipticity of the positive band at 275 nm band doubled, while that of the negative band at 240 nm decreased slightly. These changes are consistent with the alteration of the helical structure of B-DNA in the presence of **1**. Significantly, no induced CD signal was observed for the bound naphthalimide. An induced signal would be expected if it were groove-bound to the DNA as has previously been reported for its unsubstituted analogue **2**.[8e] While these CD results do not explicitly demonstrate that **1** binds to DNA *via* intercalation, they clearly show that the interaction (particularly in light of the results obtained in the LD-measurements) alters the secondary structure of DNA significantly. These results might also support our objective that the pyridinium moiety is also essential to achieving high binding affinity for DNA *via* electrostatic interactions.

Thermal denaturation studies. The influence of **1** on the thermal stability of *st*-DNA was next investigated by monitoring the temperature induced change in absorbance at 260 nm arising from the conversion of double stranded DNA to the single stranded DNA.

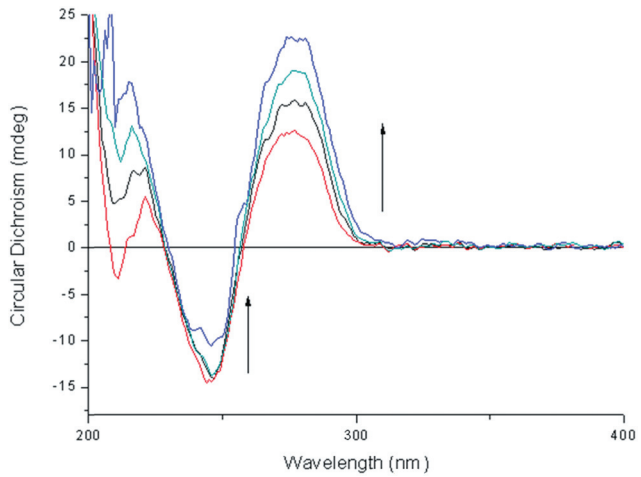

Fig. 5 The CD spectra of *st*-DNA (150 μM) in 10 mM phosphate buffer in presence of **1** at varying P/D ratios: 0 (—), 2.5 (—), 10 (—), 20 (—).

In the presence of **1** (P/D = 10), stabilisation of *st*-DNA was indicated by a 5° increase of the DNA melting temperature of *st*-DNA in 10 mM buffer solution (Fig. 6). It is perhaps significant that the extent of stabilisation is smaller than the effect observed for well-established intercalators such as ethidium bromide. However such moderate stabilization has been observed for other mono-naphthalimide based DNA intercalators previously and perhaps suggests a weaker intercalation interaction of **1**.[5,20,34]

The thermal denaturation profile of the synthetic polynucleotide poly(dA–dT)$_2$ recorded in the presence of **1** shows that **1** stabilises poly(dA–dT)$_2$ (ΔT_m = 12 °C) to a much greater extent than it does *st*-DNA, which contains 58% AT basepairs. This is indicative of a higher affinity of **1** towards AT rich sequences. (Unfortunately due to the high melting temperature of poly(dG–dC)$_2$ (~90 °C) in 10 mM phosphate buffer, it was not possible to study the thermal melting of this polynucleotide in the presence of **1**.)

UV-visible measurements. The binding of **1** with *st*-DNA was investigated from the changes in absorption of **1** in 10 mM phosphate buffer solution at pH 7.0 (Fig. 7a). In the presence of *st*-DNA, a large hypochromicity and *ca.* 10 nm red shift is observed in the ICT absorption band, accompanied by a single isosbestic point at *ca.* 480 nm for all DNA/**1** (P/D) concentrations suggesting the presence of only two spectroscopically distinct species.

The absorbance data were fitted to the non-cooperative binding model of McGhee–von Hippel to determine the intrinsic binding constant (K) and the binding site size (n) (inset Fig. 7a

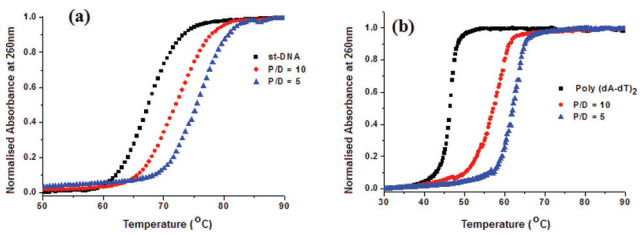

Fig. 6 Melting profile of (a) *st*-DNA and (b) poly(dA–dT)$_2$ in absence of **1** (■) and in presence of **1** (◆) (P/D = 10), (▲) (P/D = 5) in 10 mM phosphate buffer (pH 7.0).

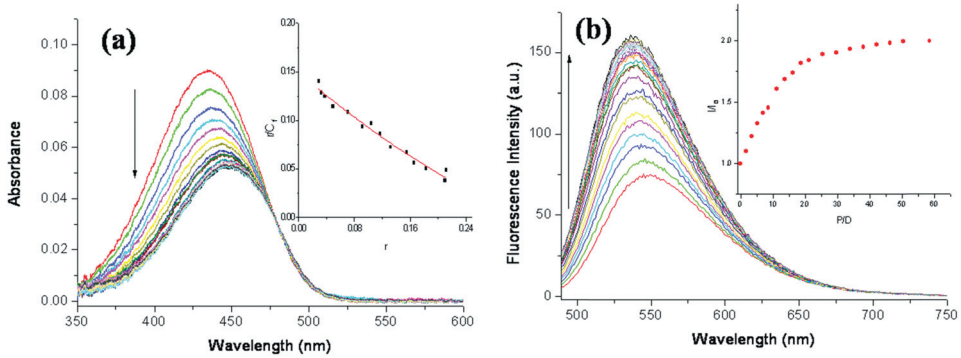

Fig. 7 (a) UV-vis spectra of **1** (7.2 μM) in the presence of increasing concentration of *st*-DNA (0–780 μM) in 10 mM phosphate buffer (pH 7.0); Inset: plot of r/C_f *vs.* r (■) and the best fit of the data (—) using the McGhee–von Hippel model. (b) Steady state emission of **1** (7.2 μM) in presence of increasing concentration of *st*-DNA (0–780 μM) (λ_{ex} = 480 nm) in 10 mM phosphate buffer (pH 7.0); Inset: plot of I/I_0 *vs.* DNA nucleotide phosphate/ligand (P/D).

Table 4 Summary of binding parameters obtained from the absorption spectra of **1** in presence of *st*-DNA in 10 mM phosphate buffer solution containing 0, 50, 100 mM NaCl

NaCl (mM)	% Hypo	$\Delta\lambda_{max}$ (nm)	K ($\times 10^5$ M^{-1})	n (bp)
0	44	12	1.85 ± 0.05	2.65 ± 0.22
50	41	12	0.64 ± 0.08	3.83 ± 0.32
100	36	12	0.26 ± 0.01	4.49 ± 0.12

and Table 4).[35] In the 10 mM phosphate buffer solution the intrinsic binding constant for the association of **1** with *st*-DNA was found to be *ca.* 1.85×10^5 M^{-1}, which is comparable to the affinity of phenothiazine dyes for DNA.[36] Notably this is an order of magnitude higher than that seen for the unsubstituted analogue **2**, demonstrating once more the importance of the 4-amino moiety and ICT character of **1**.[8] Similar DNA binding affinity has recently been reported by Qian and co-workers for thio-heterocyclic rings fused naphthalimides.[5]

To investigate the role of electrostatic interaction in the binding process, the binding of **1** with *st*-DNA was investigated in the presence of increasing NaCl concentration. An overall decrease in the magnitude of binding constant was observed with increasing ionic strength of the buffer, indicating significant contribution of electrostatic interaction in the ligand binding process (Table 4). This suggests that in the addition of the intercalation binding mode of the naphthalimide moiety, the pyridinium part plays a significant role in the overall binding affinity of **1** for DNA.

Fluorescence studies. In parallel with the absorption spectra, the steady state emission spectra of **1** were measured upon increasing concentration of *st*-DNA (Fig. 7b). It was found that the fluorescence emission of **1** was enhanced in the presence of *st*-DNA by a factor of two with a concomitant blue shift in λ_{max} of *ca.* 5 nm. This enhancement in fluorescence of **1** probably results from a decreased rate of non-radiative decay of the excited state due both to increased rigidity and the less polar nature of the binding site.

Time resolved emission measurements were also undertaken and these studies showed that in the presence of *st*-DNA, the emission decay of **1** is consistent with a bi-exponential process with a short component of τ_1 = 3.73 ns (30%) and a longer lived component of τ_2 = 9.23 ns (70%) at a P/D of 100, Table 5, which presumably represents two different localization of **1** within the DNA helix.

Interaction of 1 with synthetic polynucleotides

UV-visible absorption studies. It has been demonstrated above that **1** has a high affinity for DNA and that binding causes significant changes in its photophysical properties. As we showed earlier that complexing of **1** to AMP leads to increased excited state lifetime while GMP causes a partial quenching, it was of interest to study the behaviour of **1** in the presence of the synthetic polynucleotides poly(dA–dT)$_2$ and poly(dG–dC)$_2$.

As before the changes in the UV-vis absorption spectra of **1** with increasing concentration of poly(dA–dT)$_2$ and poly(dG–dC)$_2$ were monitored (Fig. 8a and 8b, respectively). Addition of

Table 5 Summary of binding parameters obtained from the absorption and fluorescence spectra of **1** in the presence of *st*-DNA, poly(dA–dT)$_2$ and poly(dG–dC)$_2$ in 10 mM phosphate buffer solution (pH 7)

	st-DNA	Poly(dA–dT)$_2$	Poly(dG–dC)$_2$
λ_{max} (Abs) (nm)	447	447	445
$\Delta\lambda_{max}$ (nm)	+12	+12	+10
% Hypo	44	49	52
K ($\times 10^5$ M^{-1})	1.85 ± 0.05	5.15 ± 0.07	0.82 ± 0.02
n (bp)	2.65 ± 0.22	2.54 ± 0.12	3.62 ± 0.09
λ_{max} (Flu) (nm)	547	547	544
$\Delta\lambda_{max}$ (nm)	−5	−5	−8
I/I_0	2	2	0.7[a]
τ_1 (ns)	3.7 (30%)	3.1 (6%)	1.5 (51%)
τ_2 (ns)	9.2 (70%)	9.9 (94%)	3.7 (49%)

[a] Fluorescence intensity after correcting for the absorbance decrease at 435 nm.

either polynucleotide results in large hypochromicity and a significant red shift in the ICT absorption band of **1**. In the case of poly(dA–dT)$_2$, a single isosbestic point was observed at 480 nm for the entire polynucleotide concentration range (Fig. 8a). By contrast for poly(dG–dC)$_2$ (Fig. 8b) an isosbestic point was observed (at 480 nm) only at low concentration of the polynucleotide ([poly(dG–dC)$_2$/[ligand] ≈ 3) indicating the possible existence of more than one bound form of ligand at higher concentration. The equilibrium binding constants values for the association of **1** with polynucleotides were determined as described above, from the fit of the absorbance data to non-cooperative model of McGhee and von Hippel and are summarized in Table 5. This shows that **1** exhibits a very much higher affinity for poly(dA–dT)$_2$. It may be noted that this behaviour contrasts with the lack of sequence preference for the unsubstituted compound **2**.[8e]

Fluorescence studies. The variation in the steady state emission intensity of **1** in the presence of increasing concentration of poly(dA–dT)$_2$ is shown in Fig. 8c. At high concentration of poly(dA–dT)$_2$, the emission intensity of **1** was approximately doubled, with a 5 nm blue shift similar to that observed for the titration of **1** with *st*-DNA. Time resolved emission measurements revealed that in the presence of poly(dA–dT)$_2$ at a P/D = 30 a long lived component with τ = 9.9 ns (94%) is observed corresponding to the bound form of **1** (Table 5).

As can be seen in Fig. 8d, the excited state behaviour of **1** with poly(dG–dC)$_2$ is strikingly different from that seen for poly(dA–dT)$_2$ or *st*-DNA, as the fluorescence is partially quenched rather than enhanced. Thus in the presence of poly(dG–dC)$_2$, the emission intensity of **1** is reduced by *ca.* 30% after correcting for the absorbance decrease at 435 nm. The fluorescence intensity plot (inset on Fig. 8d) again reveals the marked difference in the binding affinities for the two synthetic polynucleotides (note the different P/D scales in Fig. 8c and 8d). Time resolved measurements in the presence of excess poly(dG–dC)$_2$ (at P/D = 105) showed that the fluorescence of **1** decays by a bi-exponential process with τ_1 = 1.5 ns (51%) and τ_2 = 3.8 ns (49%), so that the observed average singlet state lifetime of **1** bound to poly(dG–dC)$_2$ remained practically unchanged from the free ligand. This behaviour may be contrasted with what was found for 5′-GMP

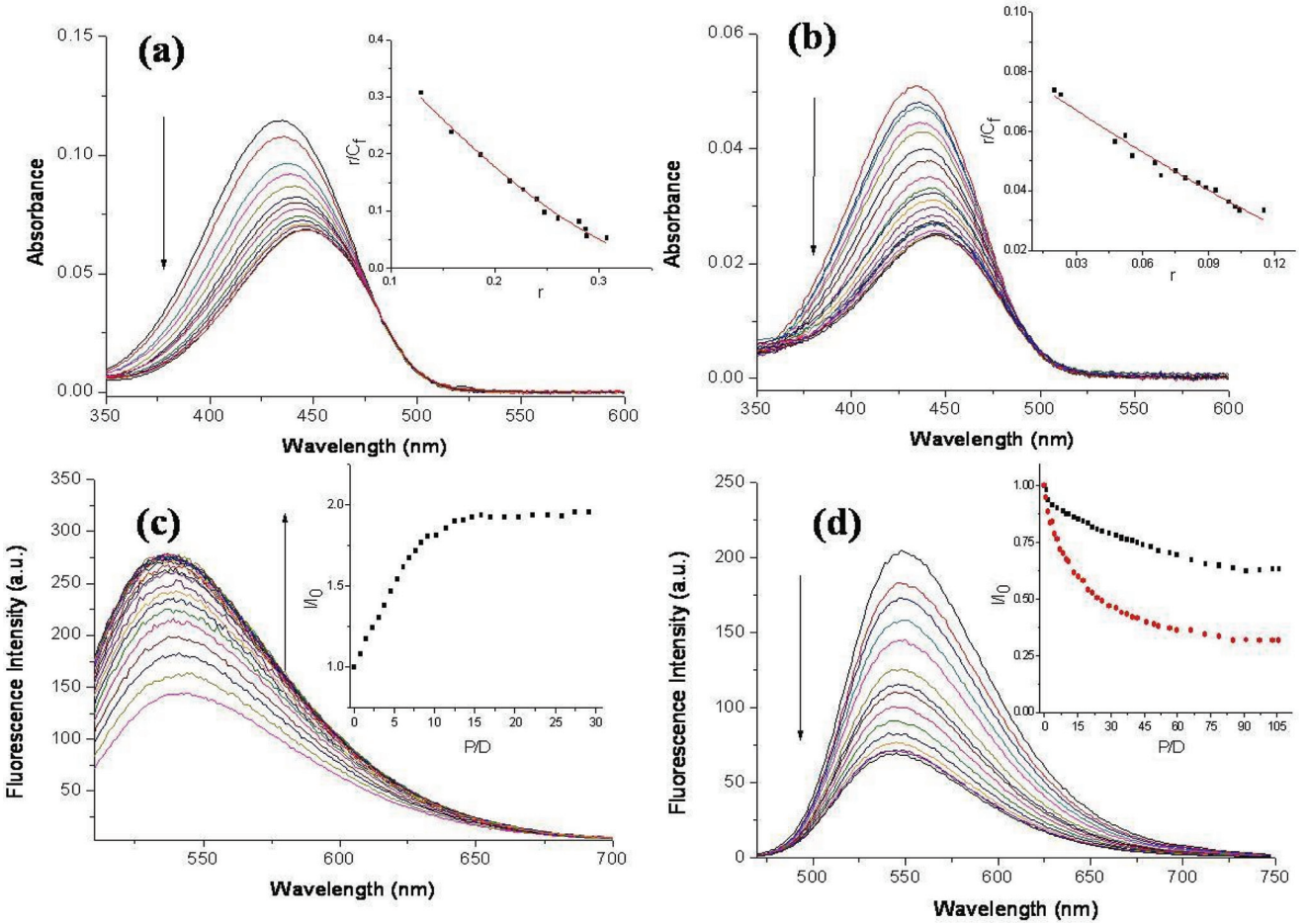

Fig. 8 The UV-vis absorption spectra of (a) **1** (7.0 μM) in presence of increasing concentration of poly(dA–dT)$_2$ (0–265 μM); (b) **1** (4.0 μM) in presence of increasing concentration of poly(dG–dC)$_2$ (0–410 μM); Inset a and b: plot of r/C_f *vs.* r and best fit (—) to McGhee–von Hippel model for poly(dA–dT)$_2$ and poly(dG–dC)$_2$ respectively; (c) **1** (7.0 μM) in presence of poly(dA–dT)$_2$ (0–265 μM) (λ_{ex} = 480 nm); (d) **1** (4.0 μM) in presence of increasing concentration of poly(dG–dC)$_2$ (0–410 μM) (λ_{ex} = 435 nm) in 10 mM phosphate buffer (pH 7.0). Inset c and d: Inset c: plot of I/I_0 *vs.* P/D for poly(dA–dT)$_2$; and poly(dG–dC)$_2$ respectively for poly(dG–dC)$_2$: (●) fluorescence intensity not corrected for absorbance decrease at λ_{ex} = 435 nm; (■) the fluorescence intensity decrease after correcting for the absorbance decrease at 435 nm.

(Table 3) where no longer-lived emission was observed and with that of poly(dA–dT)$_2$, where a much longer-lived component was detected. It is probable that two conflicting trends are operative for the singlet excited state of **1** bound to poly(dG–dC)$_2$. Firstly it is expected that there should be an increase in lifetime due to location within the non-aqueous and more rigid environment of the polynucleotide. However this will be balanced by a reduction in the excited state lifetime because of photo-induced electron transfer (PET) from guanine to the excited naphthalimide, as found with 5′-GMP.

Conclusions

This study shows that the cationic 4-amino-1,8-naphthalimide derivative **1**, which possesses a pyridinium moiety, binds strongly to DNA and synthetic polynucleotides. Linear dichroism and the other spectroscopic studies are consistent with the compound binding by intercalating between the base-pairs of polynucleotide. It is also likely that the pyridinium moiety binds electrostatically within the groove and possibly with the phosphate group of the DNA. The strong interaction between the naphthalimide ring and the purine bases is further demonstrated by the complexation with the mononucleotides 5′-AMP and 5′-GMP.

1 shows a strong preference to bind to A–T regions of DNA, as is demonstrated by the six times larger binding constant determined for poly(dA–dT)$_2$ than for poly(dG–dC)$_2$. The similar emission enhancement in both double-stranded *st*-DNA and in poly(dA–dT)$_2$ strongly suggests that in the natural DNA the intercalator also seeks out AT sequences. It is also notable that thermal denaturation experiments show that binding of **1** to poly(dA–dT)$_2$ causes a significantly higher stabilisation of the double-stranded form than is found for natural DNA, indicative of a thermodynamically stronger interaction with such alternating AT sequences. This could indicate that compounds such as **1** might therefore have a medicinal role for targeting AT rich DNA, as is for example found in the genome of the malaria parasite *P. falciparum*.[37]

It is interesting to note that **1** behaves quite differently in many respects to the analogous unsubstituted compound **4**, which McMasters and Kelly have shown locates in the minor groove of double stranded DNA with the binding predominantly

governed by the electrostatic interactions between negatively charged phosphate backbone of DNA and positively charged pyridinium group of the ligand.[8e] Surprisingly that compound does not show a preference for AT sequences, as might be expected for a groove binder. Another difference between the two compounds is that the singlet excited state of the unsubstituted compound **2** is quenched by both adenine and guanine, presumably indicative of the more oxidising nature of its excited state (due at least in part to its higher excited state energy). In the case of the amino-derivative **1** its singlet excited state clearly must have a reduction potential too low to oxidise adenine but sufficient to form the guanine radical cation (or possibly guanine radical). We have carried out preliminary picosecond transient absorption measurements to look for evidence for this electron transfer process for **1** in the presence of 20 mM GMP.[38] Although bleaching and transient absorption bands characteristic of the singlet excited state of **1** were observed and found to decay with a lifetime of 0.7 ± 0.1 ps, no new transient species were observed suggesting that back electron transfer is very rapid. Further studies are required and will be the subject of a later paper. We are also currently commencing a full biological evaluation of **1** and related compounds, which includes evaluating their cellular uptake, localisation studies, where the green emission of **1** will be capitalised on, as well as carrying out detail cytotoxic and mechanistic studies.

Experimental details

All the solvents used for photophysical studies were spectroscopic grade. Freshly distilled acetonitrile was used for quantum yield measurement. Deuterated solvents for NMR were purchased from Apollo Ltd. Millipore-purified water was used in DNA related work. The mononucleotides AMP, GMP, CMP and TMP, *st*-DNA and the synthetic polynucleotides poly(dA–dT)$_2$ and poly(dG–dC)$_2$ were obtained from Sigma Aldrich as their sodium salts. The DNA concentration (in nucleotide base) was determined spectrophotometrically using ε_{260} of 6.0×10^3 M^{-1} cm^{-1}. The concentrations of the polynucleotide stock solutions were determined using ε_{254} of 8.4×10^3 M^{-1} cm^{-1} and ε_{260} of 6.6×10^3 M^{-1} cm^{-1} for poly(dG–dC)$_2$ and poly(dA–dT)$_2$, respectively (per mole of nucleotide). All other chemicals were obtained from Sigma-Aldrich or Fluka and were used without further purification.

Infrared spectra were recorded on a Perkin Elmer Spectrum 100 FT-IR spectrophotometer. Melting points were determined using an Electrothermal IA9000 digital melting point apparatus. NMR spectra were recorded using a Bruker Advance III spectrometer, operating at 400 MHz for ^{1}H NMR and 100 MHz for ^{13}C NMR. Shifts were referenced relative to the internal solvent signals. Electrospray mass spectra were recorded on a Mass Lynx NT V 3.4 on a Waters 600 controller connected to a 996 photodiode array detector with HPLC grade methanol, water or acetonitrile as carrier solvents. All accurate masses are quoted to ≤5 ppm.

Spectroscopic measurements

UV-vis absorption spectra. These were recorded on a Varian Carry 50 spectrophotometer. All the spectroscopic measurements were carried out in quartz cuvettes (10 mm × 10 mm). 10 mM phosphate buffer of pH 7.0 was made up by mixing portions of 1 M stock solutions of Na_2HPO_4 and NaH_2PO_4. All solutions were prepared fresh prior to measurement. The association constants, K for nucleotides was determined from the slope of Scatchard plot (see ESI† for details).[27]

For the thermal denaturation studies, semi-micro UV-vis cuvettes were used (path length of 1 cm and window width of 4 mm, from Starna). The temperature-based measurements were obtained using a Cary temperature controller in conjunction with the Varian Cary 300 UV-vis spectrometer. The temperature was ramped from 30–90 °C at a rate of 0.5 °C min^{-1}. All solutions were thoroughly degassed before the experiment.

Fluorescence measurements. Steady-state fluorescence spectra were recorded on a Varian Cary Eclipse spectrofluorimeter. Fluorescence titrations, were carried out using optically dilute solutions (absorbance < 0.1) following the same procedure as described for UV-vis titrations using slit widths 5 nm for both excitation and emissions. Fluorescence quantum yields were measured using dilute solutions (absorbance <0.05) against fluorescein in 0.1 N NaOH solution (Φ = 0.9).[39] Fluorescence lifetimes were measured and analysed using Fluorolog 3 time correlated single photon counting apparatus with a Nanoled (λ_{ex} = 458 nm) used as the excitation source. Emission decays were recorded at 550 nm using slit width of 2 nm. All the decay traces were corrected for instrument response using a dilute solution of colloidal silica. In the absence of any mononucleotides, DNA or polynucleotides, decay kinetic of **1** was analysed by monoexponential model. In the presence of mononucleotides or polynucleotides, decay traces were best described by biexponential functions. Goodness of the fit was determined from the χ^2 value (1.0–1.2) and the average residual distributions.

Linear dichroism measurements. Flow oriented linear dichroism studies of were performed on a Jasco J-815 CD spectrometer fitted with a Dioptica Scientific Ltd Linear Dichroism 2 apparatus. For an oriented sample, linear dichroism is defined as the differential absorption of light polarised parallel (A_{par}) and perpendicular (A_{per}) to a reference axis (eqn (2))[33]

$$LD = A_{par} - A_{per} \quad (2)$$

Long flexible polymers such as peptides or DNA are usually oriented by the technique of flow orientation. In this technique, the molecules are oriented by shear force generated by a flow gradient in the solution flowing between the narrow gap between a spinning cell and a stationary cylindrical rod.

Quantitative information about the orientation of a chromophore with respect to the reference axis can be obtained from reduced LD (LD^r) as described in eqn (3) below,

$$LD^r = \frac{LD}{A} = \frac{A_{par} - A_{per}}{A} = \frac{3}{2}S(3\cos^2\alpha - 1) \quad (3)$$

where, A is the absorbance of the sample under isotropic condition (*i.e.* no orientation), S refers to the orientation factor (S = 1 for perfectly oriented sample, S = 0 for random orientation) and α is the angle between the transition dipole of the chromophore and the reference axis. The magnitude of S provides

information about structural changes in the macromolecule such as lengthening, stiffening, bending *etc*.

Circular dichroism measurements. CD spectra were recorded on a Jasco J810 spectropolarimeter. CD titrations were carried out by adding aliquots of solution of **1** to solution of *st*-DNA (150 μM) in 10 mM phosphate buffer at varying P/D.

Synthesis of *N*-(2-hydroxy ethyl)-4-nitro-1,8-naphthalimide (3)[21]

4-Nitro-1,8-naphthalic anhydride (2.034 g, 8.365 mmol) was suspended in dry ethanol and ethanol amine (0.5 ml) was added dropwise. The mixture was refluxed for 24 h under an argon atmosphere and cooled to room temperature. The desired product was separated by filtration, washed with cold ethanol and obtained as a dark brown solid (1.8 g, 75%). m.p. 157–160 °C (ref. 21, 157–160 °C); HRMS: 309.0488 ([M + Na]$^+$. $C_{14}H_{10}N_2O_5$ requires 309.0487); δ_H (400 MHz, d_6-DMSO), 8.65 (1H, d, J = 8.5 Hz, Ar–H7), 8.56 (1H, d, J = 8.0 Hz, Ar–H5), 8.52 (2H, m. Ar–H2, Ar–H3), 8.05 (1H, t, J = 8.0 Hz, Ar–H6), 4.85 (1H, t, J = 6.0 Hz, OH), 4.14 (2H, t, J = 6.5 Hz, CH_2), 3.64 (2H, q, J = 6.0 Hz, CH_2); δ_C (100 MHz, d_6-DMSO), 166.2 (C═O), 164.4 (C═O), 151.16 (C), 133.8 (CH), 132.2 (CH), 131.7 (CH), 130.8 (CH), 130.4 (C), 128.8 (C), 126.4 (CH), 124.9 (C), 124.8 (C), 59.8 (CH_2), 44.37 (CH_2). ν_{max}(neat sample)/cm^{-1}: 3516.46 (m, O–H stretch), 3011.6 (w, C–H asym. stretch), 2943.2 (w, C–H sym. stretch), 1691.52 (s, C═O stretch), 1579.99 (s, NO_2 asym. stretch), 1321.88 (s, NO_2 sym stretch).

Synthesis of *N*-(2-hydroxy ethyl)-4-amino-1,8-naphthalimide (4)

Compound **4** was synthesised by catalytic hydrogenation of **3** (1.00 g, 3.494 mmol) in DMF using a Parr hydrogen shaker apparatus at 3 atm pressure in the presence of 10% Pd/C catalyst until the hydrogen consumption ceased. The reaction mixture was filtered through celite and washed with DMF. The filtrate and washings were concentrated under reduced pressure and the product was precipitated as an orange solid from ice (0.812 g, 90%). m.p. 260–262 °C (ref. 70 261–263 °C); HRMS: 279.0748 ([M + Na]$^+$ $C_{14}H_{12}N_2O_3$ requires 279.0746). δ_H (400 MHz, d_6-DMSO), 8.62 (1H, d, J = 8.5 Hz, Ar–H7), 8.43 (1H, d, J = 7.5 Hz, Ar–H2), 8.20 (1H, d, J = 8.5 Hz, Ar–H5), 7.65 (1H, dd, J = 7.5 Hz and 8.0 Hz, Ar–H6), 7.44 (2H, s, –NH_2), 6.85 (1H, d, J = 8.0 Hz, Ar–H3), 4.80 (1H, t, J = 6.0 Hz, OH), 4.11 (2H, t, J = 6.5 Hz, CH_2), 3.57 (2H, q, J = 6.5 Hz, CH_2); δ_C (100 MHz, d_6-DMSO), 163.9 (C═O), 163.0 (C═O), 152.6 (C), 133.9 (CH), 130.9 (CH), 129.7 (C), 129.2 (CH), 123.9 (CH), 121.8 (C), 119.3 (C), 108.1 (CH), 107.6 (C), 57.9 (CH_2), 41.3 (CH_2). ν_{max}(neat sample)/cm^{-1}: 3437.71 (m, N–H stretch), 3349.47 (m, O–H stretch), 2925.20 (w, C–H asym. stretch), 2895.73 (w, C–H sym. stretch), 1667.78 (m, C═O stretch).

Synthesis-(2-(*N*-pyridinium)-ethyl)-4-amino-1,8-naphthalimide (1)

A mixture of **4** (0.8 g, 3.12 mmol) and *p*-toluene sulfonyl chloride (0.65 g, 3.91 mmol) were stirred in pyridine at 60 °C for 20 h and then refluxed for 4 days. The resulting precipitate was filtered and washed with DCM followed by purification using silica flash column chromatography using $CH_3CN : H_2O : NaCl$ (sat.) (88 : 11 : 1). The product was precipitated as PF_6^- salt using ammonium hexafluorophosphate. The solid was dissolved in minimum amount of MeOH and treated with DOWEX-1×8–200 ion exchange resin to convert the product into the chloride form. The product was obtained as an orange-yellow solid after removal of excess MeOH under reduced pressure (0.60 g, 60%). m.p. degraded at T > 250 °C; HRMS: 319.1233 ([M + H]$^+$. $C_{19}H_{16}N_2O_3$ requires 319.1243); δ_H (600 MHz, d_6-DMSO) 9.13 (2H, d, J = 5.6 Hz, H15), 8.67 (1H, d, J = 8.2 Hz, Ar–H5), 8.59 (1H t, J = 7.6 Hz, H17), 8.33 (1H, d, J = 7.3Hz, Ar–H7), 8.07 (3H, m, H16, Ar–H2), 7.63 (1H, t, J = 8.0, Ar–H6), 7.59 (2H, s, NH_2), 6.83 (1H, d, J = 8.6 Hz, Ar–H3), 4.94 (2H, t, J = 4.9 Hz, CH_2), 4.57 (2H, t, J = 4.5 Hz, CH_2); δ_C (150 MHz, d_6-DMSO), 164.4 (C═O), 163.3 (C═O), 153.5 (C), 146.2 (CH), 145.7 (CH), 134.5 (CH), 131.6 (CH), 130.3 (C), 130.0 (CH), 128.2 (CH), 124.3 (CH), 121.6 (C), 119.7 (C), 108.6 (CH), 107.0 (C), 60.2 (CH2), 40.6 (CH2). ν_{max}(neat sample)/cm^{-1}: 3375.42 (w, N–H stretch), 2920.58 (w, C–H asym. stretch), 2872.49 (w, C–H sym. stretch), 1679.93 (m, C═O stretch).

Acknowledgements

Financial support of Science Foundation Ireland (SFI) for RFP 2006, RFP2007, RFP 2009 and PRTLI for Cycle 4 funding to CSCB is acknowledged. JAK thanks IRCSET for a postdoctoral fellowship. We would like to thank particularly Dr John O'Brien and Dr Martin Feeney for their help with NMR and MS, respectively and Professor Mike Towrie, Dr Ian Clark and Dr Greg Greetham of the Ultrafast Laboratory of the STFC Rutherford Appleton Laboratory for the picosecond transient absorption measurements.

References

1 (*a*) L. H. Hurley, *Nat. Rev. Cancer*, 2002, **2**, 188; (*b*) S. Neidle and D. E. Thurston, *Nat. Rev. Cancer*, 2005, **5**, 285.
2 (*a*) P. A. Keane and J. M. Kelly, *Photochem. Photobiol. Sci.*, 2011, **10**, 1578; (*b*) J. G. Vos and J. M. Kelly, *Dalton Trans.*, 2006, 4869; (*c*) E. M. Tuite and J. M. Kelly, *J. Photochem. Photobiol., B*, 1993, **21**, 103.
3 (*a*) R. B. P. Elmes, M. Erby, S. M. Cloonan, S. J. Quinn, C. D. Williams and T. Gunnlaugsson, *Chem. Commun.*, 2011, **47**, 686; (*b*) D. Griffith, M. P. Morgan and C. J. Marmion, *Chem. Commun.*, 2009, 6735; (*c*) J. Andersson, S. Li, P. Lincoln and J. Andréasson, *J. Am. Chem. Soc.*, 2008, **130**, 11836.
4 (*a*) P. F. Bousquet, M. F. Brana, D. Conlon, K. M. Fitzgerald, D. Perron, C. Cocchiaro, R. Miller, M. Moran, J. George, X. D. Qian, G. Keilhauer and C. A. Romerdahl, *Cancer Res.*, 1995, **55**, 1176; (*b*) M. F. Brana, M. Cacho, A. Ramos, M. T. Dominguez, J. M. Pozuelo, C. Abradelo, M. F. Rey-Stolle, M. Yuste, C. Carrasco and C. Bailly, *Org. Biomol. Chem.*, 2003, **1**, 648; (*c*) M. F. Brana, M. Cacho, M. A. Garcia, B. de Pascual-Teresa, A. Ramos, M. T. Dominguez, J. M. Pozuelo, C. Abradelo, M. F. Rey-Stolle, M. Yuste, M. Banez-Coronel and J. C. Lacal, *J. Med. Chem.*, 2004, **47**, 1391; (*d*) M. Lv and H. Xu, *Curr. Med. Chem.*, 2009, **16**, 4797; (*e*) L. Ingrassia, F. Lefranc, R. Kiss and T. Mijatovic, *Curr. Med. Chem.*, 2009, **16**, 1192.
5 (*a*) X. Qian, Y. Li, Y. Xu, Y. Liu and B. Qu, *Bioorg. Med. Chem. Lett.*, 2004, **14**, 2665; (*b*) Y. Li, Y. Xu, X. Qian and B. Qu, *Tetrahedron Lett.*, 2004, **45**, 1247; (*c*) I. Ott, Y. Xu, J. Liu, M. Kokoschka, M. Harlos, W. S. Sheldrick and X. Qian, *Bioorg. Med. Chem.*, 2008, **16**, 7107; (*d*) Q. Yang, P. Yang, X. Qian and L. Tong, *Bioorg. Med. Chem. Lett.*, 2008, **18**, 6210; (*e*) Z. Chen, X. Liang, H. Zhang, H. Xie, J. Liu, Y. Xu,

W. Zhu, Y. Wang, X. Wang, S. Tan, D. Kuang and X. Qian, *J. Med. Chem.*, 2010, **53**, 2589; (*f*) Z. Li, Q. Yang and X. Qian, *Bioorg. Med. Chem. Lett.*, 2005, **15**, 3143.
6 (*a*) I. Saito, M. Takayama, H. Sugiyama, K. Nakatani, A. Tsuchida and M. Yamamoto, *J. Am. Chem. Soc.*, 1995, **117**, 6406; (*b*) I. Saito, M. Takayama and S. Kawanishi, *J. Am.Chem. Soc.*, 1995, **117**, 5590; (*c*) S. M. T. Matsugo, K. Yamaguchi, T. Mori and I. Saito, *Nucleic Acids Res. Symp. Ser.*, 1991, **21**, 109.
7 (*a*) T. Takada, K. Kawai, S. Tojo and T. J. Majima, *J. Phys. Chem. B*, 2004, **108**, 761; (*b*) K. Kawai, Y. Osakada, E. Matsutani and T. Majima, *J. Phys. Chem. B*, 2010, **114**, 10195.
8 (*a*) J. E. Rogers, B. Abraham, A. Rostkowski and L. A. Kelly, *Photochem. Photobiol.*, 2001, **74**, 521; (*b*) S. McMasters and L. A. Kelly, *J. Phys. Chem. B*, 2006, **110**, 1046; (*c*) J. E. Rogers and L. A. Kelly, *J. Am. Chem. Soc.*, 1999, **121**, 3854; (*d*) J. E. Rogers, S. Weiss and L. A. Kelly, *J. Am. Chem. Soc.*, 2000, **122**, 427; (*e*) S. McMasters and L. A. Kelly, *Photochem. Photobiol.*, 2007, **83**, 889.
9 R. M. Duke, E. B. Veale, F. M. Pfeffer, P. E. Kruger and T. Gunnlaugsson, *Chem. Soc. Rev.*, 2010, **39**, 3936.
10 (*a*) T. Gunnlaugsson, P. E. Kruger, T. C. Lee, R. Parkesh, F. M. Pfeffer and G. M. Hussey, *Tetrahedron Lett.*, 2003, **44**, 6575; (*b*) T. Gunnlaugsson, T. C. Lee and R. Parkesh, *Org. Biomol. Chem.*, 2003, **1**, 3265; (*c*) R. M. Duke and T. Gunnlaugsson, *Tetrahedron Lett.*, 2007, **48**, 8043; (*d*) R. Parkesh, T. C. Lee and T. Gunnlaugsson, *Org. Biomol. Chem.*, 2007, **5**, 310; (*e*) E. B. Veale and T. Gunnlaugsson, *J. Org. Chem.*, 2008, **73**, 8073; (*f*) E. B. Veale, G. M. Tocci, F. M. Pfeffer, P. E. Kruger and T. Gunnlaugsson, *Org. Biomol. Chem.*, 2009, **7**, 3447.
11 (*a*) Z. Xu, X. Qian and J. Cui, *Org. Lett.*, 2005, **7**, 3029; (*b*) Z. Xu, K. H. Baek, H. N. Kim, J. Cui, X. Qian, D. R. Spring, I. Shin and J. Yoon, *J. Am. Chem. Soc.*, 2009, **132**, 601.
12 Z. Xu, S. Kim, H. N. Kim, S. J. Han, C. Lee, J. S. Kim, X. Qian and J. Yoon, *Tetrahedron Lett.*, 2007, **48**, 9151.
13 Z. Xu, J. Yoon and D. R. Spring, *Chem. Commun.*, 2010, **46**, 2563.
14 D. Wang, X. Zhang, C. He and C. Duan, *Org. Biomol. Chem.*, 2010, **8**, 2923.
15 (*a*) A. P. d. Silva, H. Q. N. Gunaratne, J. L. Habib-Jiwan, C. P. McCoy, T. E. Rice and J. P. Soumillion, *Angew. Chem., Int. Ed. Engl.*, 1995, **34**, 1728; (*b*) A. P. de Silva, H. Q. Nimal Gunaratne and T. Gunnlaugsson, *Tetrahedron Lett.*, 1998, **39**, 5077.
16 (*a*) E. Tamanini, A. Katewa, L. M. Sedger, M. H. Todd and M. Watkinson, *Inorg. Chem.*, 2009, **48**, 319; (*b*) E. Tamanini, K. Flavin, M. Motevalli, S. Piperno, L. A. Gheber, M. H. Todd and M. Watkinson, *Inorg. Chem.*, 2010, **49**, 3789.
17 (*a*) F. M. Pfeffer, A. M. Buschgens, N. W. Barnett, T. Gunnlaugsson and P. E. Kruger, *Tetrahedron Lett.*, 2005, **46**, 6579; (*b*) F. M. Pfeffer, M. Seter, N. Lewcenko and N. W. Barnett, *Tetrahedron Lett.*, 2006, **47**, 5241.
18 Y. Li, L. Cao and H. Tian, *J. Org. Chem.*, 2006, **71**, 8279.
19 G. J. Ryan, S. Quinn and T. Gunnlaugsson, *Inorg. Chem.*, 2007, **47**, 401.
20 (*a*) E. B. Veale and T. Gunnlaugsson, *J. Org. Chem.*, 2010, **75**, 5513; (*b*) E. B. Veale, D. O. Frimannsson, M. Lawler and T. Gunnlaugsson, *Org. Lett.*, 2009, **11**, 4040.
21 S. Chatterjee, S. Pramanik, S. U. Hossain, S. Bhattacharya and S. C. Bhattacharya, *J. Photochem. Photobiol., A*, 2007, **187**, 64.
22 Y. Q. Gao and R. A. Marcus, *J. Phys. Chem. A*, 2002, **106**, 1956.
23 D. Yuan and R. G. Brown, *J. Phys. Chem. A*, 1997, **101**, 3461.
24 (*a*) A. Pardo, J. M. L. Poyato, E. Martin, J. J. Camacho, D. Reyman, M. F. Brana and J. M. Castellano, *J. Photochem. Photobiol., A*, 1989, **46**, 323; (*b*) A. Pardo, J. M. L. Poyato, E. Martin, J. J. Camacho and D. Reyman, *J. Lumin.*, 1990, **46**, 381.
25 S. Saha and A. Samanta, *J. Phys. Chem. A*, 2002, **106**, 4763.
26 (*a*) R. Jin and K. J. Breslauer, *Proc. Natl. Acad. Sci. U. S. A.*, 1988, **85**, 8939; (*b*) D. A. Barawkar and K. N. Ganesh, *Nucleic Acids Res.*, 1995, **23**, 159.
27 G. Scatchard, *Ann. N. Y. Acad. Sci.*, 1949, **51**, 660.
28 (*a*) D. A. Deranleau, *J. Am. Chem. Soc.*, 1969, **91**, 4044; (*b*) D. A. Deranleau, *J. Am. Chem. Soc.*, 1969, **91**, 4050.
29 I. V. Sazanovich, E. P. Petrov and D. A. Deranleau, *J. Am. Chem. Soc.*, 1969, **91**, 4044.
30 V. S. Chirvony, V. A. Galievsky, N. N. Kruk, B. M. Dzhagarov and P. Y. Turpin, *J. Photochem. Photobiol., B*, 1997, **40**, 154.
31 C. Prunkl, M. Pichlmaier, R. Winter, V. Kharlanov, W. Rettig and H. A. Wagenknecht, *Chem.–Eur. J.*, 2010, **16**, 3392.
32 R. Badugu, *J. Fluoresc.*, 2005, **15**, 71.
33 B. Nordén, A. Rodger and T. Dafforn. *Linear and Circular Dichroism*, RSC Publishing, 2010.
34 F. Li, J. Cui, L. Guo, X. Qian, W. Ren, K. Wang and F. Liu, *Bioorg. Med. Chem.*, 2007, **15**, 5114.
35 J. D. McGhee and P. H. von Hippel, *J. Mol. Biol.*, 1974, **86**, 469.
36 E. Tuite and J. M. Kelly, *Biopolymers*, 1995, **35**, 419.
37 M. J. Gardner, N. Hall, E. Fung, O. White, M. Berriman, R. W. Hyman, J. M. Carlton, A. Pain, K. E. Nelson and S. Bowman, *et al.*, *Nature*, 2002, **419**, 49.
38 S. Banerjee, X.-Z. Sun, M. W. George, I. Clark, G. Greetham, M. Towrie, T. Gunnlaugsson and J. M. Kelly, unpublished results.
39 J. Olmsted, *J. Phys. Chem.*, 1979, **83**, 2581.